Published in final edited form as:
Arterioscler Thromb Vasc Biol. 2012 January ; 32(1): 33–41. doi:10.1161/ATVBAHA.111.235200.

The scaffolding protein EBP50 promotes vascular smooth muscle cell proliferation and neointima formation by regulating Skp2 and p21^{cip1}

Gyun Jee Song, **Stacey Barrick**, **Kristen L. Leslie**, **Philip M. Bauer**, **Veronica Alonso**, **Peter A. Friedman**, **Nathalie M. Fiaschi-Taesch**, and **Alessandro Bisello**
Departments of Pharmacology and Chemical Biology (GJS, SB, KLL, VA, PAF and AB), Surgery (PMB), Vascular Medicine Institute (AB and PMB) and the Division of Endocrinology, Department of Medicine (NFT). University of Pittsburgh School of Medicine

Abstract

Objective—The Ezrin-Radixin-Moesin-Binding Phosphoprotein 50 (EBP50) is a scaffolding protein known to regulate ion homeostasis in the kidney and intestine. Previous work showed that EBP50 expression increases after balloon injury in rat carotids. This study was designed to determine the role of EBP50 on vascular smooth muscle cells (VSMC) proliferation and the development of neointimal hyperplasia.

Methods and Results—Wire injury was performed in wild type (WT) and EBP50 knockout (KO) mice. Two weeks after injury, neointima formation was 80% lower in KO than in WT mice. Proliferation of KO VSMC was significantly lower than WT cells and overexpression of EBP50 increased VSMC proliferation. Akt activity and expression of S-phase kinase protein 2 (Skp2) decreased in KO cells resulting in the stabilization of the cyclin-dependent kinase inhibitor, p21^{cip1}. Consequently, KO cells were arrested in G0/G1 phase. Consistent with these observations, p21^{cip1} was detected in injured femoral arteries of KO but not WT mice. No differences in apoptosis between WT and KO were observed.

Conclusions—EBP50 is critical for neointima formation and induces VSMC proliferation by decreasing Skp2 stability, thereby accelerating the degradation of the cell cycle inhibitor p21^{cip1}.

Keywords

proliferation; smooth muscle; EBP50; Skp2; p21^{cip1}

Neointimal hyperplasia is a common complication of atherosclerosis and surgical vascular interventions, particularly angioplasty. Although it is clear that neointima formation following arterial injury originates from several cellular processes, including the initial inflammatory response, increased matrix production and migration of vascular smooth muscle cells (VSMC), the proliferation of VSMC is a major contributing factor [1]. Consequently, several studies examined how manipulation of the expression of molecules involved in cell cycle progression affects neointimal hyperplasia. Of particular interest in this respect are the cyclin-dependent kinase inhibitors p21^{cip1} and p27^{kip1}.

Corresponding Author: Alessandro Bisello, Department of Pharmacology and Chemical Biology, University of Pittsburgh School of Medicine, E1358 Biomedical Science Tower, 200 Lothrop Street, Pittsburgh PA 15261, USA. Tel: 412-648-7347 Fax: 412-648-2229 alb138@pitt.edu.

Disclosures
N.F.T. is coinventor on aUnited States patent application no. 20050261183. N.F.T. has a financial interest in Vasculostatin LLC. All other authors have nothing to disclose.

Studies in animal models clearly demonstrated that increased expression of $p21^{cip1}$ in vessels decreases the progression and severity of neointima formation following injury. $p21^{cip1}$ is undetectable in uninjured human and porcine arteries but its expression increases following injury and inversely correlates with VSMC proliferation [2]. Adenoviral delivery of $p21^{cip1}$ inhibits neointimal thickening in rats and pigs [2, 3]. Moreover, $p21^{cip1}$ mediates the anti-proliferative effect of nitric oxide on VSMC [4]. However, two studies show that reduction of $p21^{cip1}$ does not increase neointimal hyperplasia in animal models [5, 6].

Similar to $p21^{cip1}$, $p27^{kip1}$ exerts important effects on disease progression. Overexpression of $p27^{kip1}$ in pig arteries reduced intima formation by 50% [7]. Increased expression of $p27^{kip1}$ attenuates neointima formation [7] and expression of a dominant negative form of Skp2 inhibits intimal hyperplasia by increasing $p27^{kip1}$ [8]. The up-regulation of $p27^{kip1}$ accounts, at least in part, for the remarkable inhibition observed upon adenoviral delivery of a parathyroid hormone-related protein (PTHrP) devoid of the nuclear localization signal [9].

The Ezrin-Radixin-Moesin-Binding Phosphoprotein 50 (EBP50), also known as NHERF1, is a cytoplasmic adaptor protein involved the regulation of a variety of membrane receptors, channels and transporters [10]. EBP50 contains two tandem PDZ motifs that mediate protein-protein interactions [11]. In addition, EBP50 possesses a C-terminal merlin-ezrin-radixin-moesin binding motif that tethers the protein to the cytoskeleton [11]. EBP50 is highly expressed in the kidney and the small intestine, where it exerts important regulatory functions on electrolyte transporters. The role of EBP50 on vascular function is largely unknown. We showed that in rat carotid arteries EBP50 expression is restricted to the endothelium and the adventitia with little (but detectable) expression in VSMC. However, EBP50 expression increases during neointima formation following arterial injury and its expression inhibits the anti-proliferative effect of the parathyroid hormone type 1 receptor [12], suggesting that this adaptor protein may contribute to neointimal hyperplasia.

The studies reported here establish important effects of EBP50 in the response of VSMC to injury. Specifically, EBP50 is critical for neointima formation and regulates VSMC proliferation by decreasing the stability of the cell cycle inhibitor $p21^{cip1.}$

Materials and Methods

Detailed methodologies for femoral artery injury, cell culture and transfection, proliferation and fluorescence-activated cell sorting assays, immunohistochemicalstaining and microscopy analysis, Western blot analysis, RT-PCR, and statistical methodsare described in the supplemental methods.

Experimental animals and surgeries

Animal studies were performed on 10 week-old wild type (WT) C57BL/6 mice and EBP50 knockout (KO) littermates. Injury was performed with a 0.014” guide wire passed within the femoral artery 3 times. The right femoral artery was used as a control uninjured artery. Femoral arteries were removed 2 weeks after surgery. All animal procedures were approved by the University ofPittsburgh Institutional Animal Care and Use Committee.

Immunofluorescence and immunohistochemistry

Femoral arteries (both control and injured) were excised from WT and KO mice, fixed with 4% paraformaldehyde and embedded in OCT Tissue-Tek (Sakura Finetek). Sections were analyzed by immunofluorescence or immunohistochemistry using antibodies against α-actin, CD31, EBP50, Ki67, $p21^{cip1}$, and $p27^{kip1}$. For morphometric analysis, frozen femoral artery sections from WT and KO mice were selected at 100 μm intervals and stained using an Elastic Stain Kit (Sigma). Images were analyzed with the Image J software (National

Institutes of Health). Immunofluorescence analysis of cultured cells was performed as described [12, 13].

Primary VSMC culture and transfection

Primary VSMC were isolated from abdominal aortic explants and cultured in Dulbecco's modified eagle media (DMEM) containing 10% fetal bovine serum (FBS) in 5% CO_2 at 37°C. All experiments were performed with cells between passages3 and 15. Cells were transfected with siRNA for EBP50 and $p21^{cip1}$ (0.1 μM) using DharmaFECT Duo transfection reagent(Dharmacon, Thermo Scientific) and used for experiments 72 h after transfection. Yellow-fluorescent protein (YFP)-tagged EBP50 was introduced in primary VSMC by electroporation. Lentiviral shRNA vectors specific to mouse EBP50 and GFP-expression control lentivirus were prepared by the Lentiviral Facility at the University of Pittsburgh Cancer Institute. Aliquots of virus were used to infect exponentially growing cells. Cells were used 72 hours after infection.

Western blot analysis, immunoprecipitation, quantitative RT-PCR and proliferation assays were performed essentially as described [12, 13].

Results

Role of EBP50 on neointima formation

The observation that EBP50 expression increases after endoluminal injury [12] suggests that it contributes to neointimal hyperplasia. To determine directly if this is the case, wire injury was performed in 10 week-old WT and KO male littermate mice. As shown in Figure 1A and B, exuberant neointima formed in WT mice (top panels) two weeks after injury. In contrast, neointima formation was significantly reduced in KO mice (lower panels). The histomorphometric parameters of the injured vessels are shown in Figure 1D. The neointimal area in WT mice was significantly larger than in KO mice, whereas the areas of the media were not different. Consequently, KO mice displayed an 80% reduction in neointima/media ratio compared to WT mice (2.54 ± 0.58 in WT mice vs. 0.53 ± 0.25 in KO mice, p=0.02, N=5) (Figure 1C).

To better characterize the cellular composition of the vessels, control and injured femoral arteries from WT and KO mice were immunostained for CD31 (to visualize endothelial cells) and α-smooth muscle actin (to visualize smooth muscle cells). No major differences were observed in uninjured vessels from WT and KO mice (Figure 1B, left panels). Two weeks after angioplasty, the neointima in WT and KO vessels was predominantly composed of cells expressing α-smooth muscle actin (Figure 1B in green) and a complete endothelial lining was observed (Figure 1B in red). Cells in the adventitia did not express α-smooth muscle actin, compatible with the predominant presence of fibroblasts. The expression of EBP50 in injured vessels was determined by immunofluorescence (Figure 1E and F). Consistent with previous observations in rat carotid arteries [12], EBP50 expression in the intima of injured femoral arteries was significantly higher than the media (ratio intima/media 3.2±0.3, p<0.004, N=4). A similar increase was determined in the adventitia (ratio adventitia/media 4.3±1.3, p<0.03, N=4).

EBP50 affects VSMC proliferation

The preceding observations raise the possibility that EBP50 contributes to neointimal hyperplasia by increasing VSMC proliferation, a key cellular event leading to neointima formation. VSMC proliferation in vivo following injury was determined by immunodetection of Ki67 (Figures 1G, H and I). The percentage of Ki67-positive cells in the intima was significantly reduced in vessels from KO mice compared to WT vessels

(Figure 1H). The number of Ki67-positive cells in the adventitia of WT and KO arteries was not significantly different (Figure 1I). To further characterize the effect of EBP50 on VSMC proliferation, we used primary VSMC isolated from WT and KO littermates. Western Blot analysis verified that EBP50 was expressed in WT cells but not in KO cells (Figure 2A). Thymidine incorporation assays and cell counting demonstrated that proliferation of KO cells was significantly lower than that of WT cells (Figure 2B and C). Similarly, the proliferation of WT cells was significantly reduced by inhibition of EBP50 expression with siRNA (Figure 2D). Conversely, increasing expression of EBP50 (by electroporation) increased WT VSMC proliferation (Figure 2E). To determine which cell cycle phase is affected by EBP50, the cell cycle distribution of WT and KO cells grown in 10% FBS was determined by fluorescence-activated cell sorting analysis. As shown in Figure 3A and Supplemental Figure IA, WT cells display a cell cycle distribution with 56% G_0/G_1, 25% S, and 19% G_2/M. In contrast, KO cells display a distribution of 79% G_0/G_1 ($p<0.04$ vs. WT), 10% S ($p<0.02$ vs. WT), and11% G_2/M ($p<0.05$ vs. WT). These experiments indicate that the absence of EBP50 causes cell cycle arrest in G_0/G_1, with consequent inhibition of cell proliferation.

EBP50 regulates $p21^{cip1}$ expression

Next, the expression of the critical regulators of the G_1-S transition was determined in WT and KO cells. Western Blot analysis indicated equal expression of cyclin E and cyclin D1 (Supplemental Figure IB). Similarly, the expression of cdk4 was unchanged in WT and KO cells. A small, not statistically significant, reduction in cdk2 and cyclin D3 expression was observed in KO cells (Supplemental Figure IB). In striking contrast, the expression of the cyclin-dependent kinase inhibitor $p21^{cip1}$ was 8-fold higher in KO cells compared to WT (Figure 3B and C). Identical observations were made in independent preparations from two other mice (Supplemental Figure IC). Quantitative RT-PCR showed that the mRNA levels of $p21^{cip1}$ were similar in WT and KO cells (Figure 3D), suggesting that EBP50 regulates $p21^{cip1}$ expression post-translationally. Consistent with this interpretation, the expression of p53, a well known upstream regulator of $p21^{cip1}$ transcription, was unchanged in KO cells (Figure 3B). In addition, the regulation of $p21^{cip1}$ expression by EBP50 was fully recapitulated in CHO cells following recombinant expression of myc-tagged $p21^{cip1}$ and EBP50 under the control of CMV promoters (Supplemental Figure ID). The expression of $p27^{kip1}$, another inhibitor of the G1-S transition, was equal in WT and KO cells (Figure 3B and D), indicating that the regulation of $p21^{cip1}$ by EBP50, and the consequent effects on cell cycle progression, are specific. To determine if the expression of $p21^{cip1}$ is critical for the different proliferation of WT and KO VSMC, its expression in KO cells was inhibited by siRNA. This treatment resulted in an 80% reduction in $p21^{cip1}$ protein (Figure 3E). Decreasing $p21^{cip1}$ expression significantly accelerated KO cell proliferation (Figure 3E), indicating that the expression level of this cell cycle inhibitor is sufficient to regulate SMC growth [14].

Immunofluorescence analysis of KO VSMC demonstrated high expression and clear nuclear localization of $p21^{cip1}$ (Supplemental Figure IIA). In contrast, $p21^{cip1}$ expression was significantly reduced in WT VSMC (Supplemental Figure IIA). Total levels of $p21^{cip1}$ increased in both WT and KO cells upon treatment with the proteasome inhibitor MG132. The increase in WT cells was significantly higher than in KO cells, suggesting an increased degradation rate of $p21^{cip1}$ in WT cells (Supplemental Figure IIB and C). Similarly, the total levels of $p27^{kip1}$ increased upon treatment with MG132, but the effect was similar in WT and KO cells (Supplemental Figure IIC). To determine whether the expression of EBP50 correlates with $p21^{cip1}$ degradation, $p21^{cip1}$ was visualized in KO VSMC transfected with YFP-EBP50. $p21^{cip1}$ was detected in the nucleus of more than 90% of KO VSMC. In contrast, only 50% of cells expressing YFP-EBP50 were also positive for $p21^{cip1}$

(p=0.0001) (Supplemental Figure III). Collectively, these experiments show that $p21^{cip1}$ levels are lower in cells expressing EBP50, and that EBP50 increases degradation of $p21^{cip1}$. Indeed, the half-life of $p21^{cip1}$ (determined in the presence of cyclohexamide) was reduced in WT cells compared to KO cells (45±8 min in WT cells vs. 82±16 min in KO cells) (Figure 4A and Supplemental Figure IV).

EBP50 regulates Skp2 expression

The reduced degradation of $p21^{cip1}$ in EBP50KO cells suggests that EBP50 may regulate the activity of the Skp1/Cullin-1/F-box (SCF) E3-ligase responsible for $p21^{cip1}$ degradation [15]. Of particular interest is the F-box protein Skp2 that directs recognition of $p21^{cip1}$ by the SCF complex [16]. The expression of Skp2 was reduced in primary VSMC from KO mice (Figure 4B). Similar reduction in Skp2, accompanied by a corresponding increase in $p21^{cip1}$ was observed in WT cells in which EBP50 expression was inhibited by two distinct lentivirus expressing shRNA against EBP50 (Figure 4C, left panel). Conversely, expression of YFP-EBP50 in VSMC increased Skp2 and reduced $p21^{cip1}$ (Figure 4C, right panel). The relation between EBP50 and Skp2 expression was established in distinct VSMC preparations in which EBP50 expression was reduced to various degrees by shRNA. As shown in Figure 4D, a direct and significant correlation was found between the expression of EBP50 and that of Skp2 in primary VSMC. The stability of Skp2 (determined in the presence of cyclohexamide) was reduced in KO cells compared to WT cells (Figure 4E. In contrast, mRNA for Skp2 was not different in WT and KO VSMC (Figure 4F), indicating that EBP50 predominantly regulates Skp2 expression post-translationally. To determine if the expression level of Skp2 is critical to VSMC proliferation, KO VSMC were transiently transfected with Flag-Skp2. Immunofluorescence analysis showed the clear localization of Flag-Skp2 in the nucleus (Supplemental Figure V). In these cells proliferation (determined by co-staining for BrDU) was significantly increased (Figure 4G).

Collectively, these experiments show that EBP50 regulates Skp2 levels and, consequently, $p21^{cip1}$ stability. However, we found no difference in $p27^{kip1}$ expression in WT and KO cells (Figure 3B). This suggests the possibility that $p27^{kip1}$ degradation is less sensitive to modest variations in Skp2 expression than $p21^{cip1}$. Indeed, overexpression of Skp2 in KO VSMC efficiently decreased both $p21^{cip1}$ and $p27^{kip1}$ (Supplemental Figure VI).

The reduction of Skp2 expression in EBP50 KO cells prompted us to determine if, in addition to the reduction in cell proliferation, other phenotypes observed upon deletion of Skp2 [17] were also evident in upon EBP50 knockout. The body weight of EBP50 KO mice was reduced compared to WT littermates up to seven weeks of age, after which the mice were of similar size (Supplemental Figure VIIA). Skp2 null cells are enlarged compared to normal cells [17]. Consistent with these observations, EBP50 KO VSMC were larger than WT cells (Supplemental Figure VIIB).

EBP50 regulates Akt activity

Akt is a major transducer of mitogenic signals in a variety of cells[18]. Akt is activated by arterial injury and contributes to neointima formation[19, 20]. Since EBP50 regulates growth factors signaling and Akt activity in a cell-specific manner[21–26], we determine Akt activity in WT and KO VSMC. As shown in Figure 5A, serum stimulation of previously starved WT cells induced robust phosphorylation of Akt after 5 and 30 min. In contrast, the response of KO cells to the same stimulus was blunted. Similar reduction in Akt activation was determined in KO cells upon stimulation with EGF (Figure 5B). Moreover, as reported previously, EBP50 co-immunoprecipitated with Akt (Figure 5C and Supplemental Figure VIII), an interaction that potentiates Akt activation [26]. The expression and cellular localization of phosphatase and tensin homolog (PTEN), a regulator of the PI3K/Akt

pathway known to interact with EBP50 [23, 25], was not different in WT and KO VSMC (Supplemental Figure IX). Collectively, these experiments show that EBP50 potentiates Akt activity in VSMC by regulating growth factor receptor signaling and by directly interacting with Akt. Inhibition of Akt by LY294002 and Akt1/2 kinase inhibitor (AKTI) blocked VSMC proliferation both in WT and KO cells (Figure 5D). Akt inhibition was equally effective in reducing proliferation (assessed by BrDU incorporation) of naive VSMC and of cells overexpressing YFP-EBP50 (Figure 5E and Supplemental Figure X), indicating that the mitogenic action of EBP50 is Akt-dependent.

The preceding observations raise an intriguing question. In most mammalian cells, Akt regulates Skp2 expression both transcriptionally and by increasing its stability[27, 28]. The latter effect has been attributed to the direct phosphorylation of Skp2 by Akt[27, 28]. However, Akt does not phosphorylate mouse Skp227. Thus, the mechanisms by which Akt regulates Skp2 expression in mouse cells, and the possible involvement of EBP50, remain unclear. Consistent with other reports [14, 27, 28], inhibition of Akt with either LY294002 or AKTI reduced Skp2 expression in VSMC maintained in serum-supplemented media (Figure 5F), confirming the key role of Akt on Skp2 transcription. Furthermore, immunoprecipitation assays show that EBP50 constitutively interacts with Skp2 and this interaction is increased by expression of a constitutively active form of Akt (Myr-Akt) (Figure 5G). This observation suggests a possible mechanism for the observed stabilization of Skp2 in EBP50 expressing mouse cells.

EBP50 regulates $p21^{cip1}$ expression in vivo

The preceding observations in primary VSMC clearly indicate that in the absence of EBP50 the stability of $p21^{cip1}$ is increased resulting in inhibition of cell proliferation. To determine if similar regulation occurs in vivo, the expression of $p21^{cip1}$ was determined in the femoral arteries of WT and KO mice. $p21^{cip1}$ was undetectable in control uninjured vessels (Figure 6 left panels). Similarly, little expression of $p21^{cip1}$ was observed in injured vessels of WT mice. In contrast, $p21^{cip1}$ was present both in the neointima and in the adventitia of femoral arteries of KO mice two weeks after injury (Figure 6, right panels). Consistent with the findings in cells, analysis of $p27^{kip1}$ expression in WT and KO femoral arteries revealed similar expression in both control and injured vessels (Supplemental Figure XI).

VSMC growth is the balance between proliferation and apoptosis, and $p21^{cip1}$ plays important roles on both cellular events. To determine if the different expression of $p21^{cip1}$ in WT and KO mice affects VSMC survival, apoptosis in injured vessels was determined by TUNEL staining. The number of apoptotic cells in the intima and media of WT and KO vessels two weeks after injury was very low (approximately 0.25% of total cells) and not different between mice (Supplemental Figure XIIA). To assess possible differences in apoptosis upon cellular stress, TUNEL assays were performed in WT VSMC and in cells in which EBP50 expression was inhibited by shRNA following 24 h of serum starvation. Again, no differences in TUNEL staining were observed between control and shRNA-treated cells (Supplemental Figure XIIB). These observations suggest that differences in cell survival do not contribute to the reduced neointima formation in KO mice.

Discussion

The major finding in this report is the remarkable effect that the scaffolding protein EBP50 has in the development of neointimal hyperplasia following arterial injury. Two key and novel observations are presented. First, genetic ablation of EBP50 in mice results in almost complete inhibition of restenosis following endothelial denudation. Second, EBP50 exerts important effects on the cell cycle of VSMC, in particular by regulating the expression of Skp2 and the stability of the cell cycle inhibitor $p21^{cip1}$.

EBP50 is widely expressed and its function in the regulation of electrolyte transport has been well characterized in the kidney and intestine [29, 30]. The original observation that EBP50 expression increases in the neointima formed after endothelial denudation in rat carotid arteries [12], replicated here in murine femoral arteries, suggested its possible involvement in the response of VSMC to injury. The lack of neointimal hyperplasia observed in EBP50 knockoutmice is, to the best of our knowledge, the first evidence of the actions of EBP50 on vascular remodeling. The reduced cell proliferation of KO cells was accompanied by cell cycle arrest in the G_0/G_1 phase.Examination of the principal regulators of the G_1-S transition clearly indicated that the major protein affected by EBP50 is $p21^{cip1}$. $p21^{cip1}$ levels were increased in both cultured KO cells and in the injured vessels of KO mice. The role of $p21^{cip1}$ in regulating VSMC proliferation and neointima formation has been documented by several investigators. In particular, increased expression of $p21^{cip1}$ in vessels resulted in diminished hyperplasia following injury [2, 7], a result fully consistent with the observations in EBP50 KO mice. Yet, neointima formation is not increased in $p21^{cip1}$ knockout mice [5] and increased expression of the transcription factor Ying-Yang 1 inhibits neointimal hyperplasia while reducing $p21^{cip1}$ expression [6]. Collectively, these observations indicate that although $p21^{cip1}$ is competent to reduce VSMC proliferation and inhibit neointima formation, its absence does not necessarily promote these events, suggesting the existence of compensatory effects from other cell-cycle controlling proteins (such as $p27^{kip1}$). Interestingly, the regulation of $p21^{cip1}$ by EBP50 occurs entirely post-translationally. This is supported by several lines of evidence. The mRNA levels of $p21^{cip1}$ and the expression of p53, the major regulator of $p21^{cip1}$ transcription [31], are identical in WT and KO cells. The half-life of $p21^{cip1}$ was increased in KO cells compared to WT cells. Inhibition of the proteasome by MG132 increased total $p21^{cip1}$ levels in both WT and KO cells, but to a greater extent in WT cells, indicating an increased degradation of $p21^{cip1}$ in these cells. Finally, experiments in single cells indicate that EBP50 expression inversely correlates with $p21^{cip1}$ expression.

These observations indicate that EBP50 facilitates $p21^{cip1}$ degradation. This process is dependent on the action of the E3 ubiquitin ligase complex consisting of Cullin-1, Skp1 and RBX1 as well as Skp2 which regulates substrate recognition [15, 16]. We show that ablation of EBP50 induces a marked decrease in Skp2 and, consequently, stabilization of $p21^{cip1}$ in cultured cells and in vivo. Conversely, EBP50 overexpression increases Skp2 and decreases $p21^{cip1}$ levels in VSMC. Consistent with these findings, adenoviral delivery of a dominant negative form of Skp2 reduced VSMC proliferation and neointima formation in rats [8]. Several studies demonstrated that the PI3K/Akt pathway is a major regulator of Skp2 expression [14, 27, 28, 32]. Indeed, complete inhibition of Akt abrogated Skp2 expression in primary VSMC. We did not detect differences in Skp2 mRNA between WT and KO cells–possibly indicating that the level of Akt signaling in KO cells is sufficient to fully induce gene expression. However, the stability of Skp2 in WT cells was increased. Interestingly, direct phosphorylation of Skp2 by Akt, leading to cytoplasmic retention and stabilization of Skp2 [27, 28], does not occur in mice because Ser72, the site of phosphorylation, is a Gly in the murine Skp2. It should be noted that the importance of phosphorylation of Ser72 for the cellular localization of Skp2 is still controversial [33]. Our observations indicate that a different mechanism mediates Akt-dependent regulation of Skp2. The interaction between EBP50 and Skp2 and the potentiation of this interaction by a constitutively active Akt provide a possible explanation for the regulation of Skp2 stability by Akt in mouse cells. Further studies are required to establish the molecular events underlying the effect of Akt on Skp2 stability in murine systems.

EBP50 deficiency attenuates Akt activity in primary VSMC. This regulation occurs at several levels. First, EBP50 interacts constitutively with Akt and increases Akt activation[26]. Second, EBP50 increases the function of the receptors for epidermal growth factor and

platelet-derived growth factor, two major activators of Akt signaling in VSMC [21, 22]. EBP50 has been shown to regulate membrane localization, and therefore activity, of the PI3K inhibitor PTEN in glioblastoma cells [23]. However, we detected no differences in PTEN expression and localization in VSMC from WT and KO mice. It is interesting to observe that the effect of EBP50 on proliferation is remarkably tissue- and cell-specific. EBP50 is over-expressed in glioblastomas[34], hepatocellular[35] and breast carcinomas[36]. Yet, the direction of the effect of EBP50 on cell growth is variable. Although in breast cancer cells and in embryonic fibroblasts EBP50 inhibits cell proliferation [37, 38], in biliary epithelial cells, as in VSMC, EBP50 stimulates cell growth [39]. EBP50 regulates a variety of molecules involved in cell growth, including growth factor and G protein-coupled receptors, β-catenin and PTEN. Therefore, whether EBP50 stimulates or inhibits proliferation depends on the relative importance of these signaling pathways. We show here that the PI3K/Akt/Skp2/$p21^{cip1}$ is the major pathway mediating the proliferative effect of EBP50 on VSMC. In contrast, the effect of EBP50 on adventitial cells, predominantly fibroblasts, was not different between WT and KO mice.

EBP50 does not alter the regulation of $p27^{kip1}$ in VSMC, consistent with observations made in clonal rat A10 cells [12]. This finding is somewhat puzzling because, like $p21^{cip1}$, $p27^{kip1}$ is subject to regulation by Akt and ubiquitin ligase complexes [40]. We observed that $p27^{kip1}$ was actively degraded in both WT and KO cells. This suggests the possibility that $p27^{kip1}$ degradation is less sensitive to variations in Akt signaling and Skp2 expression than $p21^{cip1}$. It is important to note that in the primary cultures used in these studies neither Akt signaling nor Skp2 expression were entirely abrogated or over activated. In fact, overexpression of Skp2 in WT VSMC reduced both $p21^{cip1}$ and $p27^{kip1}$. In addition, $p21^{cip1}$ and $p27^{kip1}$ are targeted by more than one E3 ligase and by different kinases [40]. It is also possible that EBP50 regulates the ability of Skp2 to specifically recognize and discriminate substrates for degradation. Determining the exact molecular mechanisms underlying the effect of EBP50 on substrate recognition by Skp2 requires further investigation.

In summary, we describe the identification of the scaffolding protein EBP50 as a key regulator of vascular remodeling. EBP50 is required for neointima formation following endoluminal arterial injury in mice and, by controlling Skp2 expression and the stability of $p21^{cip1}$, exerts important actions on cell cycle progression of VSMC. These findings reinforce the emerging importance of scaffolding and adaptor proteins as major regulators of physiological and pathological events.

Supplementary Material

Refer to Web version on PubMed Central for supplementary material.

Acknowledgments

Funding Sources

This work was supported by the National Institutes of Health National Institute of Diabetes and Digestive and Kidney Diseases Grants DK071158 (to AB) and DK069998 (to PAF), the American Heart Association Great River Grant-in-Aid 10BGIA350005 (to GJS), and a Pilot Project Program in Hemostasis and Vascular Biology - Vascular Medicine Institute, University of Pittsburgh - supported by grants from the Institute for Transfusion Medicine and the Hemophilia Society of Western Pennsylvania (to AB). KLL is supported by the NIH pre-doctoral training grant T32GM08424.

Non-standard abbreviations

EBP50 Ezrin Binding Protein 50

KO	EBP50 knockout
RT-PCR	reverse transcriptase polymerase chain reaction
Skp2	S-phase kinase protein 2
VSMC	vascular smooth muscle cell
WT	wild type
YFP	yellow fluorescent protein

References

1. Rajagopal V, Rockson SG. Coronary restenosis: a review of mechanisms and management. Am J Med. 2003; 115:547–553. [PubMed: 14599634]
2. Yang ZY, Simari RD, Perkins ND, San H, Gordon D, Nabel GJ, Nabel EG. Role of the p21 cyclin-dependent kinase inhibitor in limiting intimal cell proliferation in response to arterial injury. Proc Natl Acad Sci U S A. 1996; 93:7905–7910. [PubMed: 8755575]
3. Chang MW, Barr E, Lu MM, Barton K, Leiden JM. Adenovirus-mediated over-expression of the cyclin/cyclin-dependent kinase inhibitor, p21 inhibits vascular smooth muscle cell proliferation and neointima formation in the rat carotid artery model of balloon angioplasty. J Clin Invest. 1995; 96:2260–2268. [PubMed: 7593612]
4. Bauer PM, Buga GM, Ignarro LJ. Role of p42/p44 mitogen-activated-protein kinase and p21waf1/^{cip1} in the regulation of vascular smooth muscle cell proliferation by nitric oxide. Proc Natl Acad Sci U S A. 2001; 98:12802–12807. [PubMed: 11592976]
5. Sata M, Takahashi A, Tanaka K, Washida M, Ishizaka N, Ako J, Yoshizumi M, Ouchi Y, Taniguchi T, Hirata Y, Yokoyama M, Nagai R, Walsh K. Mouse genetic evidence that tranilast reduces smooth muscle cell hyperplasia via a p21(WAF1)-dependent pathway. Arterioscler Thromb Vasc Biol. 2002; 22:1305–1309. [PubMed: 12171792]
6. Santiago FS, Ishii H, Shafi S, Khurana R, Kanellakis P, Bhindi R, Ramirez MJ, Bobik A, Martin JF, Chesterman CN, Zachary IC, Khachigian LM. Yin Yang-1 inhibits vascular smooth muscle cell growth and intimal thickening by repressing p21WAF1/^{Cip1} transcription and p21WAF1/^{Cip1}-Cdk4-cyclin D1 assembly. Circ Res. 2007; 101:146–155. [PubMed: 17556661]
7. Tanner FC, Boehm M, Akyurek LM, San H, Yang ZY, Tashiro J, Nabel GJ, Nabel EG. Differential effects of the cyclin-dependent kinase inhibitors p27(Kip1), p21(Cip1), and p16(Ink4) on vascular smooth muscle cell proliferation. Circulation. 2000; 101:2022–2025. [PubMed: 10790340]
8. Wu YJ, Sala-Newby GB, Shu KT, Yeh HI, Nakayama KI, Nakayama K, Newby AC, Bond M. S-phase kinase-associated protein-2 (Skp2) promotes vascular smooth muscle cell proliferation and neointima formation in vivo. J Vasc Surg. 2009; 50:1135–1142. [PubMed: 19878790]
9. Fiaschi-Taesch N, Sicari B, Ubriani K, Cozar-Castellano I, Takane KK, Stewart AF. Mutant parathyroid hormone-related protein, devoid of the nuclear localization signal, markedly inhibits arterial smooth muscle cell cycle and neointima formation by coordinate up-regulation of p15Ink4b and p27^{kip1}. Endocrinology. 2009; 150:1429–1439. [PubMed: 18845646]
10. Reczek D, Berryman M, Bretscher A. Identification of EBP50: A PDZ-containing phosphoprotein that associates with members of the ezrin-radixin-moesin family. J Cell Biol. 1997; 139:169–179. [PubMed: 9314537]
11. Weinman EJ, Hall RA, Friedman PA, Liu-Chen LY, Shenolikar S. The association of NHERF adaptor proteins with g protein-coupled receptors and receptor tyrosine kinases. Annu Rev Physiol. 2006; 68:491–505. [PubMed: 16460281]
12. Song GJ, Barrick S, Leslie KL, Sicari B, Fiaschi-Taesch NM, Bisello A. EBP50 inhibits the anti-mitogenic action of the parathyroid hormone type 1 receptor in vascular smooth muscle cells. J Mol Cell Cardiol. 2010; 49:1012–1021. [PubMed: 20843475]
13. Song GJ, Fiaschi-Taesch N, Bisello A. Endogenous parathyroid hormone-related protein regulates the expression of PTH type 1 receptor and proliferation of vascular smooth muscle cells. Mol Endocrinol. 2009; 23:1681–1690. [PubMed: 19574446]

14. Bond M, Sala-Newby GB, Wu YJ, Newby AC. Biphasic effect of $p21^{Cip1}$ on smooth muscle cell proliferation: role of PI 3-kinase and Skp2-mediated degradation. Cardiovasc Res. 2006; 69:198–206. [PubMed: 16212951]
15. Cardozo T, Pagano M. The SCF ubiquitin ligase: insights into a molecular machine. Nat Rev Mol Cell Biol. 2004; 5:739–751. [PubMed: 15340381]
16. Frescas D, Pagano M. Deregulated proteolysis by the F-box proteins SKP2 and beta-TrCP: tipping the scales of cancer. Nat Rev Cancer. 2008; 8:438–449. [PubMed: 18500245]
17. Nakayama K, Nagahama H, Minamishima YA, Matsumoto M, Nakamichi I, Kitagawa K, Shirane M, Tsunematsu R, Tsukiyama T, Ishida N, Kitagawa M, Nakayama K, Hatakeyama S. Targeted disruption of Skp2 results in accumulation of cyclin E and p27(Kip1), polyploidy and centrosome overduplication. Embo J. 2000; 19:2069–2081. [PubMed: 10790373]
18. Manning BD, Cantley LC. AKT/PKB signaling: navigating downstream. Cell. 2007; 129:1261–1274. [PubMed: 17604717]
19. Zhou RH, Lee TS, Tsou TC, Rannou F, Li YS, Chien S, Shyy JY. Stent implantation activates Akt in the vessel wall: role of mechanical stretch in vascular smooth muscle cells. Arterioscler Thromb Vasc Biol. 2003; 23:2015–2020. [PubMed: 12969991]
20. Shigematsu K, Koyama H, Olson NE, Cho A, Reidy MA. Phosphatidylinositol 3-kinase signaling is important for smooth muscle cell replication after arterial injury. Arterioscler Thromb Vasc Biol. 2000; 20:2373–2378. [PubMed: 11073840]
21. Lazar CS, Cresson CM, Lauffenburger DA, Gill GN. The Na+/H+ exchanger regulatory factor stabilizes epidermal growth factor receptors at the cell surface. Mol Biol Cell. 2004; 15:5470–5480. [PubMed: 15469991]
22. Maudsley S, Zamah AM, Rahman N, Blitzer JT, Luttrell LM, Lefkowitz RJ, Hall RA. Platelet-derived growth factor receptor association with Na(+)/H(+) exchanger regulatory factor potentiates receptor activity. Mol Cell Biol. 2000; 20:8352–8363. [PubMed: 11046132]
23. Molina JR, Morales FC, Hayashi Y, Aldape KD, Georgescu MM. Loss of PTEN binding adapter protein NHERF1 from plasma membrane in glioblastoma contributes to PTEN inactivation. Cancer Res. 70:6697–6703. [PubMed: 20736378]
24. Pan Y, Weinman EJ, Dai JL. Na+/H+ exchanger regulatory factor 1 inhibits platelet-derived growth factor signaling in breast cancer cells. Breast Cancer Res. 2008; 10:R5. [PubMed: 18190691]
25. Takahashi Y, Morales FC, Kreimann EL, Georgescu MM. PTEN tumor suppressor associates with NHERF proteins to attenuate PDGF receptor signaling. Embo J. 2006; 25:910–920. [PubMed: 16456542]
26. Wang B, Yang Y, Friedman PA. Na/H exchange regulatory factor 1, a novel AKT-associating protein, regulates extracellular signal-regulated kinase signaling through a B-Raf-mediated pathway. Mol Biol Cell. 2008; 19:1637–1645. [PubMed: 18272783]
27. Gao D, Inuzuka H, Tseng A, Chin RY, Toker A, Wei W. Phosphorylation by Akt1 promotes cytoplasmic localization of Skp2 and impairs APCCdh1-mediated Skp2 destruction. Nat Cell Biol. 2009; 11:397–408. [PubMed: 19270695]
28. Lin HK, Wang G, Chen Z, Teruya-Feldstein J, Liu Y, Chan CH, Yang WL, Erdjument-Bromage H, Nakayama KI, Nimer S, Tempst P, Pandolfi PP. Phosphorylation-dependent regulation of cytosolic localization and oncogenic function of Skp2 by Akt/PKB. Nat Cell Biol. 2009; 11:420–432. [PubMed: 19270694]
29. Shenolikar S, Voltz JW, Minkoff CM, Wade JB, Weinman EJ. Targeted disruption of the mouse NHERF-1 gene promotes internalization of proximal tubule sodium-phosphate cotransporter type IIa and renal phosphate wasting. Proc Natl Acad Sci U S A. 2002; 99:11470–11475. [PubMed: 12169661]
30. Seidler U, Singh A, Chen M, Cinar A, Bachmann O, Zheng W, Wang J, Yeruva S, Riederer B. Knockout mouse models for intestinal electrolyte transporters and regulatory PDZ adaptors: new insights into cystic fibrosis, secretory diarrhoea and fructose-induced hypertension. Exp Physiol. 2009; 94:175–179. [PubMed: 18931049]
31. Levine AJ. p53, the cellular gatekeeper for growth and division. Cell. 1997; 88:323–331. [PubMed: 9039259]

32. Barre B, Perkins ND. The Skp2 promoter integrates signaling through the NF-kappaB, p53, and Akt/GSK3beta pathways to regulate autophagy and apoptosis. Mol Cell. 38:524–538. [PubMed: 20513428]
33. Bashir T, Pagan JK, Busino L, Pagano M. Phosphorylation of Ser72 is dispensable for Skp2 assembly into an active SCF ubiquitin ligase and its subcellular localization. Cell Cycle. 9:971–974. [PubMed: 20160477]
34. Kislin KL, McDonough WS, Eschbacher JM, Armstrong BA, Berens ME. NHERF-1: modulator of glioblastoma cell migration and invasion. Neoplasia. 2009; 11:377–387. [PubMed: 19308292]
35. Shibata T, Chuma M, Kokubu A, Sakamoto M, Hirohashi S. EBP50, a beta-catenin-associating protein, enhances Wnt signaling and is over-expressed in hepatocellular carcinoma. Hepatology. 2003; 38:178–186. [PubMed: 12830000]
36. Song J, Bai J, Yang W, Gabrielson EW, Chan DW, Zhang Z. Expression and clinicopathological significance of oestrogen-responsive ezrin-radixin-moesin-binding phosphoprotein 50 in breast cancer. Histopathology. 2007; 51:40–53. [PubMed: 17593079]
37. Pan Y, Wang L, Dai JL. Suppression of breast cancer cell growth by Na+/H+ exchanger regulatory factor 1 (NHERF1). Breast Cancer Res. 2006; 8:R63. [PubMed: 17078868]
38. Kreimann EL, Morales FC, de Orbeta-Cruz J, Takahashi Y, Adams H, Liu TJ, McCrea PD, Georgescu MM. Cortical stabilization of beta-catenin contributes to NHERF1/EBP50 tumor suppressor function. Oncogene. 2007; 26:5290–5299. [PubMed: 17325659]
39. Fouassier L, Rosenberg P, Mergey M, Saubamea B, Claperon A, Kinnman N, Chignard N, Jacobsson-Ekman G, Strandvik B, Rey C, Barbu V, Hultcrantz R, Housset C. Ezrin-radixin-moesin-binding phosphoprotein (EBP50), an estrogen-inducible scaffold protein, contributes to biliary epithelial cell proliferation. Am J Pathol. 2009; 174:869–880. [PubMed: 19234136]
40. Lu Z, Hunter T. Ubiquitylation and proteasomal degradation of the p21(Cip1), p27(Kip1) and p57(Kip2) CDK inhibitors. Cell Cycle. 2010; 9:2342–2352. [PubMed: 20519948]

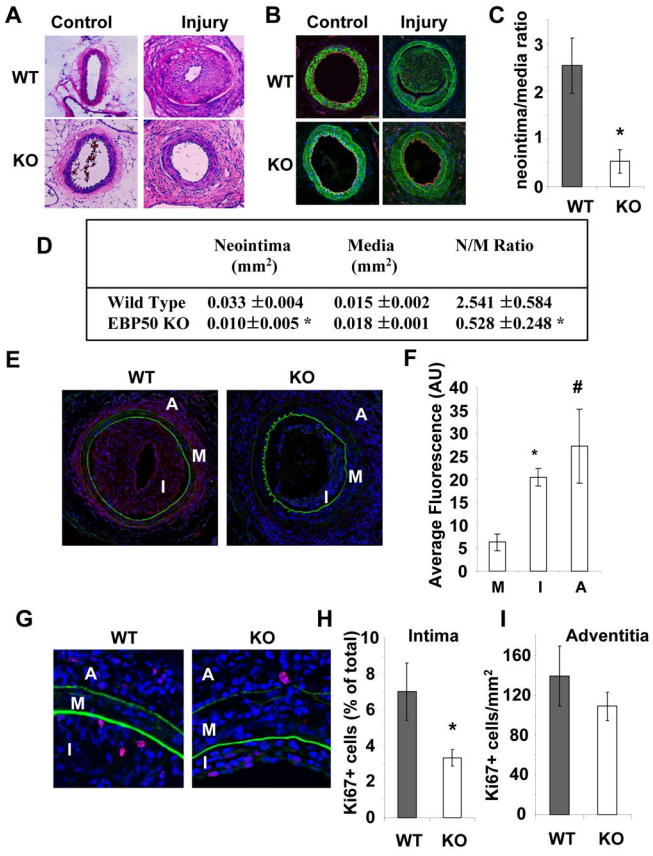

Figure 1. EBP50 is required for neointima formation

A. Sections of control and injured femoral arteries from WT and KO stained with hematoxylin and eosin. In WT mice exuberant neointima formed in two weeks (top right panel). Reduced neointimal hyperplasia was detected in KO mice (bottom right panel). Of note, the proliferative response in the adventitia is evident in both mouse strains (right panels). **B**. Sections of control and injured femoral arteries from WT and KO mice stained for α-smooth muscleactin (in green), CD31 (in red). Nuclei were visualized with DAPI (in blue). **C**. Ratio neointima/media (± standard error). *, $p<0.02$, N=5. **D**. Histomorphometric analysis of injured vessels from WT and KO mice. **E**. Sections of femoral arteries 2 weeks after injury were fixed and immunostained for EBP50 (in red). Shown in green are auto-fluorescent elastin fibers. Nuclei were visualized with DAPI (in blue). **F**.Quantification of EBP50 expression in femoral arteries following injury. Graphs show the average fluorescence intensity (± SE) of EBP50 in the media (M), intima (I) and adventitia (A) determined from sections immunostained as described above. *, $p<0.002$, #, $p<0.03$ versus media, N=4. **G**. Sections of femoral arteries 2 weeks after injury were fixed and immunostained for Ki67 (in red). Shown in green are auto-fluorescent elastin fibers. Nuclei were visualized with DAPI (in blue). **H**. Percentage of Ki67 positive cells in the intima of WT and KO vessels. *, $p<0.005$, N=5. **I**. Number of Ki67 positive cells per unit area of adventitia of WT and KO vessels.

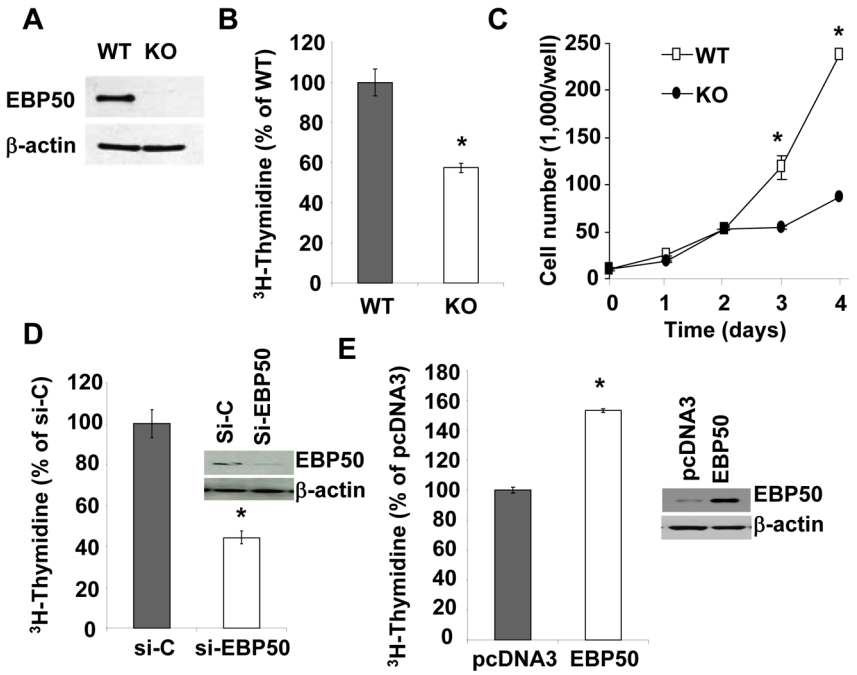

Figure 2. EBP50 induces VSMC proliferation

AEBP50 expression in WT and KO VSMC was determined by immunoblot (top panel). β-actin was used as loading control (lower panel). **B**.Proliferation of WT and KO VSMC maintained in 10% FBS determined by [^{3}H]-thymidine incorporation. *, p<0.002. **C**. Proliferation of WT and KO VSMC maintained in 10% FBS determined by cell counting. Ten thousand cells were plated on day 0 and counted at the indicated times. **C**. Proliferation of WT VSMC transfected with control siRNA (si-C) or siRNA for EBP50 (si-EBP50) determined by [^{3}H]-thymidine incorporation. *, p<0.002. Insert shows the expression of EBP50 in si-C and si-EBP50 treated cells. **C**. Proliferation of WT VSMC transfected with control plasmid (pcDNA3) or EBP50 determined by [^{3}H]-thymidine incorporation. *, p<0.0001. Insert shows the expression of EBP50 in control and EBP50-transfected cells. Data are expressed as mean ± standard error for triplicate determinations and are representative of three to five independent assays.

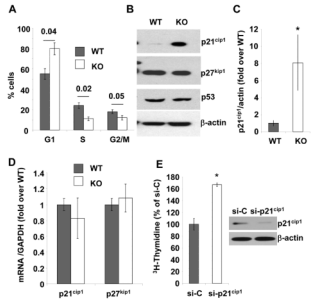

Figure 3. Effect of EBP50 on vascular smooth muscle cell cycle and p21^{cip1} expression

A. Cell cycle distribution analyzed by FACS in WT (gray bars) and KO (white bars) VSMC. The percentage ± standard error of the population of cells in G1, S and G2/M phases are derived from five independent experiments. P values for WT vs. KO are indicated. **B**. Immunoblots for p21^{cip1}, p27^{kip1} and p53 in WT and KO VSMC. β-actin was used as loading control. Blots are representative of at least five independent experiments. **C**. Quantification of the expression of p21^{cip1} in WT (gray bars) and KO (white bars) VSMC. The ratio of p21^{cip1} expression over β-actin was determined in five independent experiments. *, p<0.04. **D**.Quantitative RT-PCR for p21^{cip1} and p27^{kip1} using mRNA from WT (gray bar) and KO (white bar) VSMC. Results are presented as fold over WT ± standard error of triplicate determinations. Values were normalized relative to GAPDH. **E**. Inhibition of p21^{cip1} expression by siRNA increases VSMC proliferation. Immunoblot for p21^{cip1} in KO VSMC transfected with either control siRNA (si-C) or p21^{cip1}siRNA (si-p21^{cip1}) as indicated. β-actin is used as loading control. Proliferation of KO VSMC transfectedwith either control siRNA (si-C) or p21^{cip1} siRNA (si-p21^{cip1}) and maintained in 10% FBS determined by [^{3}H]-thymidine incorporation. Data are presented as percentage of si-C treated cells ± standard error of triplicate determinations. Similar results were obtained in two additional experiments. *, p<0.003.

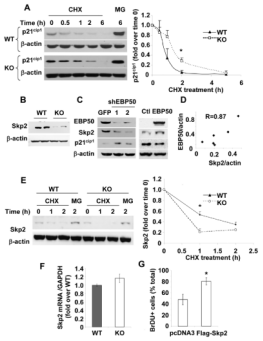

Figure 4. EBP50 regulates Skp2 and p21^{cip1} stability

A. Primary VSMC from WT (left panels) and KO (right panels) mice were treated with cyclohexamide (10 μg/ml) or MG132 (2 μM) for the indicated times. Equal amounts of proteins were analyzed by immunoblotting for p21^{cip1} and β-actin (as loading control). Data are presented as mean (± standard error) of the p21^{cip1} intensity (normalized with β-actin) relative to time zero. *, $p<0.05$, N=3. **B**. The expression of Skp2 was determined by immunoblotting in WT and KO cells as indicated. **C**. WT VSMC were infected with control adenovirus expressing GFP or two distinct shRNA against EBP50 (shEBP50 # 1 and #2) (left panel) or transfected with YFP-EBP50 (right panel). The expression of EBP50, Skp2 and p21^{cip1} was determined by immunoblotting. **D**. Correlation between EBP50 and Skp2 expression in 6 independent VSMC preparations. **E**. Primary VSMC from WT and KO mice treated as described in A were analyzed by immunoblotting for Skp2 and β-actin (as loading control). Graph shows the quantitation of three independent experiments. Data are presented as mean (± standard error) of the Skp2 intensity (normalized with β-actin) relative to time zero.*, $p<0.008$, N=4. **F**. Quantitative RT-PCR for Skp2 using mRNA from WT (gray bar) and KO (white bar) VSMC. Results are presented as fold over WT ± standard error of triplicate determinations. Values were normalized relative to GAPDH. **G**. Primary VSMC from KO mice were electroporated with control vector (pcDNA3) or Flag-Skp2 and cultured in the presence of BrDU for 16 h. Cells were fixed and stained for BrDU and Flag. The percentage of BrDU positive cells was determined from three independent experiments. *, $p=0.04$, N=3.

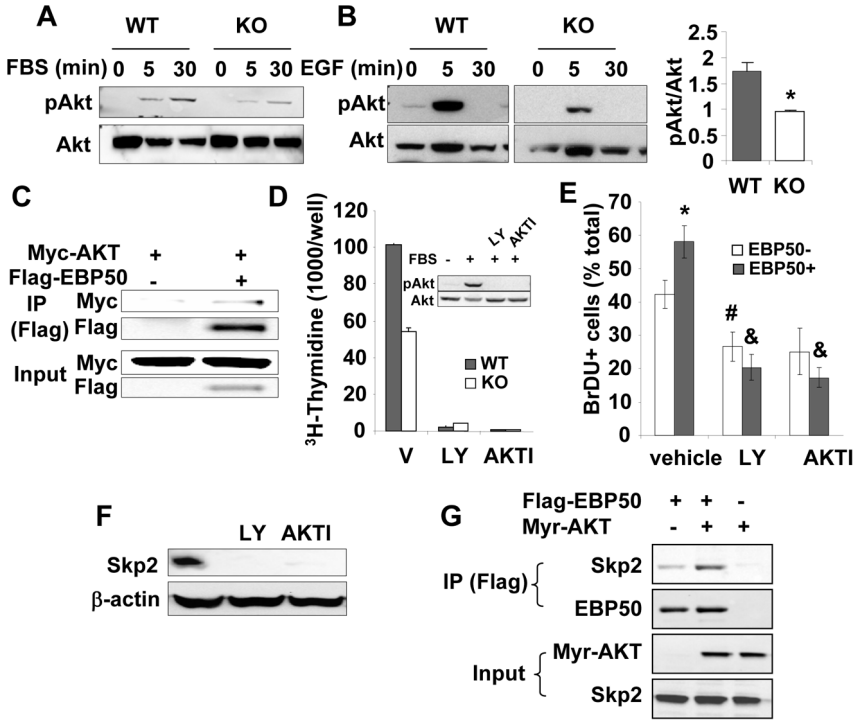

Figure 5. EBP50 ablation decreases Akt signaling and Skp2 expression

A. WT and KO VSMC were serum-starved for 16 h followed by the addition of 10% FBS for the indicate times. Phosphorylated and total Akt were determined by immunoblotting. Blots are representative of 4 independent experiments. **B**. WT and KO VSMC were serum-starved for 16 h followed by the addition 10 ng/ml EGF for the indicate times. Phosphorylated and total Akt were determined by immunoblotting. Graph shows the quantitation of 3 independent experiments. *<0.05. **C**. Primary VSMC were transiently transfected with Myc-Akt and Flag-EBP50, as indicated. Cells were lysed, and immunoprecipitation experiments were performed with anti-Flag antibody followed by SDS-PAGE and immunoblotting with anti-Flag or anti-Myc antibodies. **D**. Proliferation (determined by [^{3}H]-thymidine incorporation) of WT and KO VSMC treated without or with 10 μM LY-294002 (LY) or 5 μM AKTI for 16 h and maintained in 10% FBS. Data are expressed as mean ± standard error for triplicate determinations. Shown is also a western blot analysis of phosphorylated and total Akt in similarly treated cells. **E**. Primary VSMC from KO mice were electroporated with YFP-EBP50, treated without or with 10 μM LY-294002 (LY) or 5 μM AKTI in the presence of BrDU for 16 h. Cells were fixed and stained for BrDU. The percentage of BrDU positive non-transfected and YFP-EBP50-expressing cells was determined from three independent experiments. *, p=0.03 vs. EBP50-, #, p<0.02 vs. vehicle, &, p<0.01 vs. vehicle; N=3. **F**. VSMC maintained in 10% FBS were treated without or with 10 μM LY-294002 (LY) or 5 μM AKTI. Skp2 expression was determined by immunoblotting. β-actin was used as loading control. **G**. CHO cells were transiently transfected with constitutively active HA tagged Myr-Akt and Flag-EBP50, as indicated. Cells were lysed, and immunoprecipitation experiments were performed with anti-Flag antibody followed by SDS-PAGE and immunoblotting with anti-Flag, anti-HA or anti-Skp2 antibodies.

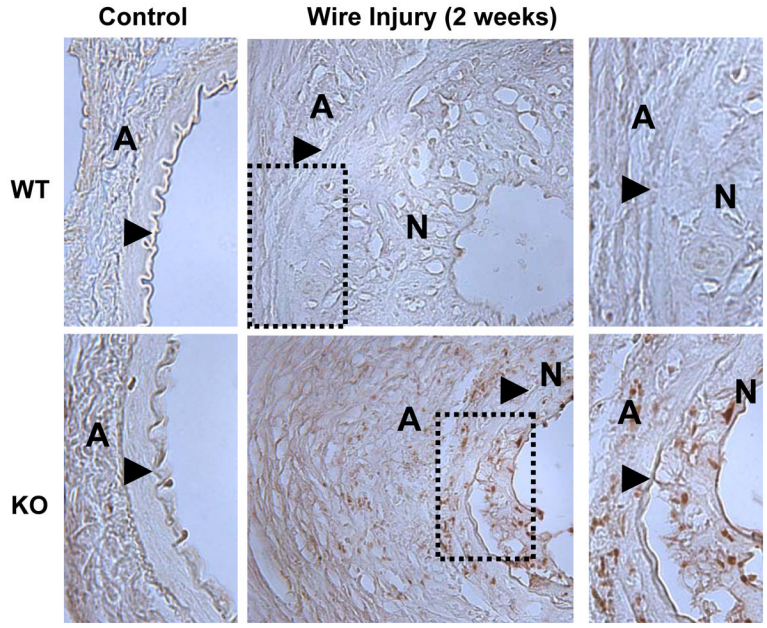

Figure 6. Expression of p21^{cip1} in mouse femoral arteries

Sections from uninjured femoral artery (left panels) or 2 weeks after wire injury (middle panels) from WT (upper panels) and KO (lower panels) mice were stained for p21^{cip1} (in brown). Shown on the right are higher magnification pictures of the dotted areas. The external elastic lamina is indicated by an arrow, N indicates the neointima and A the adventitia. The expression of p21^{cip1} is evident in femoral arteries from KO mice two weeks after injury.